Homogeneous Catalysis Hot Paper

How to cite: *Angew. Chem. Int. Ed.* **2021**, *60*, 26500–26505
International Edition: doi.org/10.1002/anie.202110910
German Edition: doi.org/10.1002/ange.202110910

Acceptorless Dehydrogenation of Methanol to Carbon Monoxide and Hydrogen using Molecular Catalysts

*Akash Kaithal, Basujit Chatterjee, Christophe Werlé, and Walter Leitner**

Dedicated to Professor Holger Braunschweig on the occasion of his 60th birthday

Abstract: *The acceptorless dehydrogenation of methanol to carbon monoxide and hydrogen was investigated using homogeneous molecular complexes. Complexes of ruthenium and manganese comprising the MACHO ligand framework showed promising activities for this reaction. The molecular ruthenium complex [RuH(CO)(BH$_4$)(HN(C$_2$H$_4$PPh$_2$)$_2$)] (Ru-MACHO-BH) achieved up to 3150 turnovers for carbon monoxide and 9230 turnovers for hydrogen formation at 150 °C reaching pressures up to 12 bar when the decomposition was carried out in a closed vessel. Control experiments affirmed that the metal complex mediates the initial fast dehydrogenation of methanol to formaldehyde and methyl formate followed by subsequent slow decarbonylation. Depending on the catalyst and reaction conditions, the CO/H$_2$ ratio in the gas mixture thus varies over a broad range from almost pure hydrogen to the stoichiometric limit of 1:2.*

Methanol is widely inferred as a crucial molecular pivot at the interface of the energy and chemical sectors.[1] It can be produced from renewable resources,[2] including direct hydrogenation of carbon dioxide.[3] It is easily stored, transported, and distributed in liquid form and hence considered as an energy storage material for fuel cells or by liberating molecular hydrogen upon reforming (Scheme 1a). The carbon atom is re-emitted in the form of carbon dioxide in these applications, ultimately closing the loop with CO_2 as a hydrogen carrier. Alternatively, one might envisage a different decomposition pathway by catalytic dehydrogenation of methanol to a mixture of hydrogen and carbon monoxide known as "syngas" (Scheme 1b). This process liberates one equivalent of H_2 less but co-generates CO as high energy and very valuable C1 building block for industrial transformations. Bulk chemicals such as acetic acid,[4] acetic anhydride,[5] as well as polyketones,[6] polycarbonates,[7] and polyurethanes,[8] require CO as feedstock, sometimes even together with MeOH. Important commodities and high-value products are produced via hydroformylation[9] and other carbonylation reactions.[10] Non-fossil technologies for syngas production such as the reverse water gas shift reaction (rWGS)[11] or co-electrolysis[12] rely mainly on the direct conversion of gaseous CO_2 with renewable energy on-site, whereas methanol dehydrogenation offers an attractive alternative to harvest stranded energy and carbon resources.

Methanol reforming to produce hydrogen and CO_2 (Scheme 1a) is well-established, and various heterogeneous and homogeneous catalysts are known for this transformation.[13] Heterogeneous catalysts typically require high temperatures (> 200 °C), whereas noble (Ru, Ir)[14] and non-noble (Fe, Mn)[15] metal-based molecular catalysts were recently established which can perform this transformation at lower temperatures. Comparably few reports deal with the dehydrogenation of methanol to gaseous CO and H_2. Mostly, gas phase processes using heterogeneous catalysts at temper-

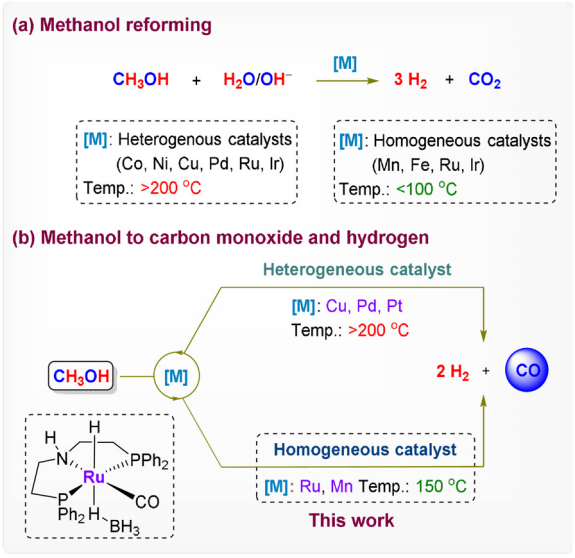

Scheme 1. a) Established process for the methanol-reforming. b) Synthesis of carbon monoxide and hydrogen gas from methanol using heterogeneous and molecular catalysts.

[*] Dr. A. Kaithal, Dr. B. Chatterjee, Dr. C. Werlé, Prof. Dr. W. Leitner
Max Planck Institute for Chemical Energy Conversion
Stiftstraße 34–36, 45470 Mülheim a.d. Ruhr (Germany)
E-mail: walter.leitner@cec.mpg.de
Dr. C. Werlé
Ruhr University Bochum
Universitätsstr. 150, 44801 Bochum (Germany)
Prof. Dr. W. Leitner
Institut für Technische und Makromolekulare Chemie, RWTH Aachen University
Worringer Weg 2, 52074 Aachen (Germany)
Supporting information and the ORCID identification number(s) for the author(s) of this article can be found under: https://doi.org/10.1002/anie.202110910.

atures around or above 200 °C were investigated.[16] Examples with homogeneous catalysts remain so far elusive, however.

Herein, we report the acceptorless dehydrogenation of methanol using molecular organometallic catalysts in the liquid phase to generate gaseous mixtures of CO and H_2 in various compositions and at elevated pressures. The study was initiated by a screening of various molecular complexes with known activities in hydrogen-transfer reactions (Table 1).[17] Reactions were carried out in stainless-steel high-pressure vessels (14 mL inner volume) using glass liners to avoid contact of the reaction mixture with the reactor wall. The metal complex (10 μmol), together with optionally 2 equivalents of NaO^{t}Bu as an activator, was dissolved in 2 mL of MeOH, and the reactor heated to 150 °C for 8 h. The gas-phase composition was analyzed using gas chromatography (experimental error ±10%), and the liquid phase was analyzed by NMR spectroscopy in selected cases. The molar amounts of the gaseous phase products are given in relation to the molar amount of metal as "turnover number (TON)" to quantify the performance of the catalytic systems for the individual products.

Using the complex Ru-MACHO-BH (**1**) in the absence of base under the screening conditions resulted in an increase of pressure reaching 12 bar at reaction temperature and maintaining 5.2 bar after cooling the reactor to room temperature. The gas-phase analysis showed the presence of 0.67 mmol of CO and 1.20 mmol of H_2, corresponding to the stoichiometric 1:2 ratio within experimental error, with only trace amounts of CO_2 (0.004 mmol). The amounts of gaseous products correspond to a TON of 67 for CO and 121 for H_2 (entry 1). The measured amounts of H_2 and CO were reproducible within maximum ±3% deviation in duplicated experiments (see SI for selected examples). The Ru complex (**3**) comprising the Milstein ligand and the Noyori-type catalyst (**4**) were also active but required base activation and proved significantly less productive (entry 3, 4). The ruthenium complex **2** and iridium catalyst $[IrCp^*Cl_2]_2$ (**5**), both known as efficient dehydrogenation catalysts, remained inactive (entry 2, 5). The manganese-based congener for Ru-complex **1**, i.e. Mn^I-MACHO-^{i}Pr (**6**) also showed high activity for CO and H_2 formation upon base activation with a TON of 53 and 98, respectively (entry 6).[18] The other Mn^I pincer complexes with triazine (**7**) or lutidine ligands (**8**) resulted in low reactivity (entry 7, 8). Heating methanol in the absence of metal complexes with or without base did not result in any formation of CO and H_2 (entry 11, 12).

Further optimization to increase the TONs was carried out with the two MACHO-type complexes **1** and **6**. While the ruthenium complex showed some activity even at 120 °C (Table 1, entries 9, 10), the standard temperature of 150 °C was maintained in the parameter variation (Table 2).

Reducing the reaction scale by using 5 μmol of complex **1** in 1 mL MeOH effectively doubled the TON values while producing the same CO/H_2 ratio (Table 2, entry 1). Decreasing the loading further to 1 μmol and extending the reaction time to 12 h again resulted in largely identical amounts of CO and H_2 in a 1:2 ratio, indicating that this corresponds to the limiting conversion under these conditions (Table 2, entry 2, 3). Lowering the loading of **1** under these conditions resulted in greatly increased TONs demonstrating the very high efficacy of this catalyst (Table 2, entry 4–6). While the relative

Table 1: Reaction optimization for the dehydrogenation of methanol to CO and H_2 using different metal complexes [M] and temperature optimization.[a]

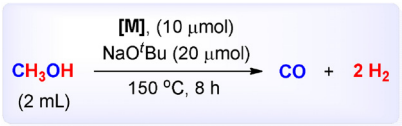

#	[M]	T [°C]	TON (CO)	TON (H_2)	TON (CO_2)	Ratio (CO:H_2)
1[b]	**1**	150	67	121	0.4	1:1.8
2[c]	**2**	150	0	4	0.1	0
3[c]	**3**	150	32	82	0.2	1:2.6
4	**4**	150	15	39	2	1:2.6
5	**5**	150	0	0	0	0
6	**6**	150	53	98	0.5	1:1.9
7	**7**	150	1	5	0.3	≈1:5
8	**8**	150	1	3	0	≈1:3
9	**1**	120	28	52	0.1	1:1.9
10	**1**	100	8	90	0.5	1:11.3
11[d]	–	150	0	0	0	0
12[e]	–	150	0	0	0	0

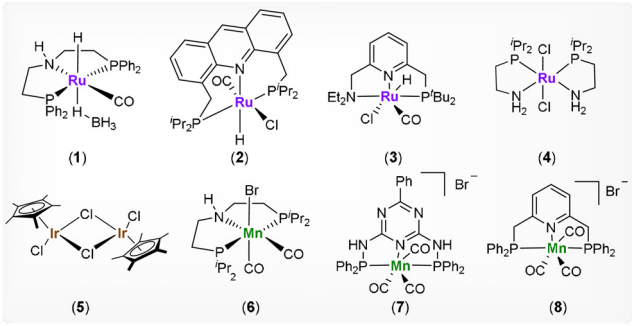

[a] All reactions were performed in a 14 mL autoclave-maximum error: ±10%. [b] No NaO^{t}Bu was used in the reaction. [c] < 1 ppm methane was observed. [d] Reaction was performed in the absence of [M] and NaO^{t}Bu. [e] Reaction was performed in the presence of only NaO^{t}Bu.

Table 2: Turnover number optimization for the dehydrogenation of methanol to CO and H_2 using complexes **1** and **6**.[a]

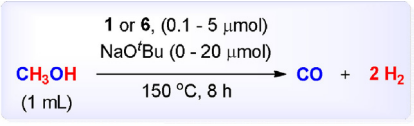

#	[M] [μmol]	NaO^{t}Bu [μmol]	TON (CO)	TON (H_2)	TON (CO_2)	Ratio (CO:H_2)
1	**1** (5)	–	129	234	1.1	1:1.8
2	**1** (1)	–	404	897	3.2	1:2.2
3[b]	**1** (1)	–	460	946	4.3	1:2.1
4	**1** (0.5)	-	705	1939	8.7	1:2.8
5	**1** (0.25)	–	1003	3918	17.7	1:3.9
6	**1** (0.1)	–	1464	8347	24.9	1:5.7
7	**6** (5)	20	88	159	0.1	1:1.8
8	**6** (2.5)	20	30	190	3.8	1:6.3
9	**6** (1)	20	4	328	17.2	1:82

[a] All reactions were performed in a 14 mL autoclave-maximum error: ±10%. [b] Reaction was performed for 12 h.

amount of H_2 vs. CO increased, the selectivity of CO vs. CO_2 decreased somewhat at the lower loadings (125:1 in entry 2 vs. 60:1 in entry 6). In the case of Mn-catalyst **6**, the total TONs also increased with lower catalyst loadings, and the selectivity shifted towards H_2 formation, leading to a ratio of CO/H_2 of 1:82 at a loading of 1 μmol in 1 mL of MeOH (Table 2, entry 7–9).

The reaction time profile for the dehydrogenation of MeOH to CO and H_2 using catalyst **1** (1 μmol in 1 mL MeOH) was determined by GC analysis of the gas phase at different time intervals (Figure 1). In the initial five minutes, only hydrogen formation took place with a TON of 55, while other gases such as CO or CO_2 were not detected. Hydrogen evolution is rapid in the first 30 minutes with an apparent turnover frequency ($TOF = TON/\Delta t$) of ca. 1200 h^{-1} ($\Delta t = 0$–30 minutes). The formation of CO sets in at this stage, albeit with an almost one order of magnitude lower rate (ca 150 h^{-1}, $\Delta t = 10$–100 minutes). After a reaction of 3 h, hydrogen evolution reached a plateau, whereas CO formation continued, albeit with an even lower rate. As time progressed, the CO/H_2 ratio approached the stoichiometric limit of 1:2 (1:2.1 after 12 h).

The plateau of the reaction indicates that the reaction reaches an equilibrium defined by the build-up of the partial pressures of the gaseous products.[17d,g] In order to demonstrate the robustness of the catalytic system, the reaction was performed for a longer period using only 0.5 μmol of complex **1** in 1 mL of MeOH, monitoring the composition of the gas phase of the reaction mixture every 12 h over a total of 84 h. The kinetic profile was largely identical to that shown in Figure 1, reaching a total TON of 3150 for CO and 9230 for H_2, with only a marginal formation of CO_2 corresponding to a TON of 41.

Monitoring the same reaction using deuterated methanol revealed a significant isotope effect (Figure 2). The initial rate for D_2 formation was with a TOF of 900 h^{-1} ($\Delta t = 0$–30 min), about 25% lower than for the hydrogen isotopomer ($k_H/k_D \approx 1.3$). The effect is even larger for CO formation, where the

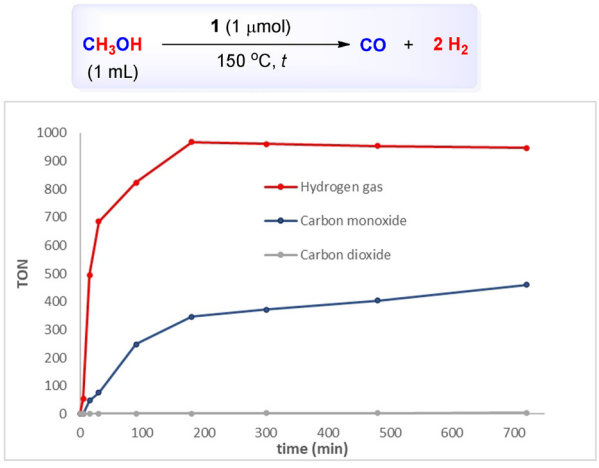

Figure 1. Turnover number/time profile based on gas chromatography of individual experiments. CH_3OH (1 mL), and Ru-complex **1** (1 μmol) were heated at 150 °C in a high-pressure reactor for the given reaction time.

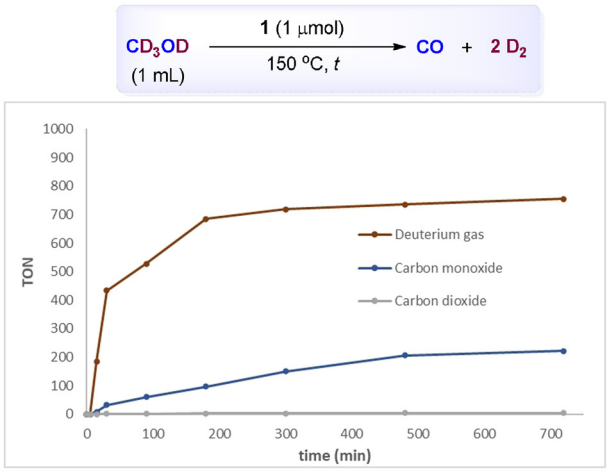

Figure 2. Turnover number/time profile based on gas chromatography of individual experiments. CD_3OD (1 mL), and Ru-complex **1** (1 μmol) were heated at 150 °C in a high-pressure reactor for the given reaction time.

apparent rate is reduced to TOF 20 h^{-1} ($\Delta t = 30$–300 min) corresponding to $k_H/k_D \approx 7.5$. These data indicate that C–H bond cleavage is involved in the rate-limiting step of both processes, albeit via a different types of intermediates and transition states.

To elucidate the potential pathways and intermediates for methanol dehydrogenation, the liquid phase was investigated by NMR spectroscopy after 12 h reaction time. The half-acetal of formaldehyde and methanol, methoxymethanol ($\delta =$ 4.61 ppm), and methylformate ($\delta = 8.01$ ppm) were detected as the only components in addition to methanol (see SI). Control experiments were conducted to investigate whether the CO liberation can occur either on the formaldehyde or formate level (Scheme 2). When paraformaldehyde was reacted with complex **1** under the same reaction conditions using toluene as a solvent, gas-phase analysis confirmed 131 TON for CO, 45 TON of H_2, and 90 TON for CO_2 (Scheme 2a). The substantial amount of CO_2 formation can be explained due to the decomposition of paraformaldehyde, which in the presence of complex **1** and water disproportionates to generate formic acid, methanol, and CO_2.[19] Methyl formate was decarbonylated very cleanly and effectively by complex **1** using *t*-amyl alcohol as solvent under otherwise identical conditions (Scheme 2b). These investigations indicate that formaldehyde and methyl formate can both serve as intermediates for the decarbonylation step. The clean and effective decarbonylation of methylformate together with the observed reaction profiles indicates that this pathway seems to be dominating at the later stage where CO formation prevails over H_2 generation.

Formation of the presumed active species **I** was confirmed by spectroscopic analysis (SI 12.5). The lability of the CO ligand in complex **I** was validated as this would be expected to be crucial for catalytic turnover. Exchange of the carbonyl ligand with ^{13}CO was confirmed by NMR, IR, and MS analysis as shown in Scheme 2c. In situ IR monitoring of complex **1** in the presence of ^{13}CO (2 bar) also showed the

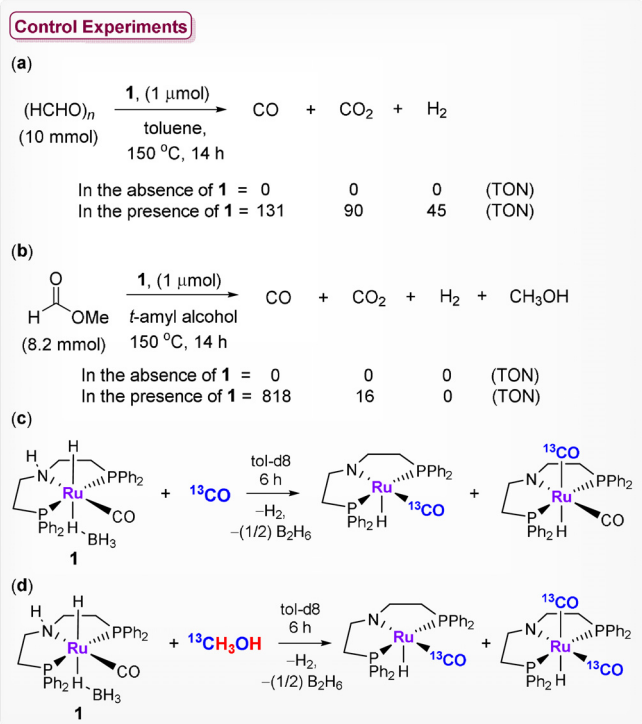

Scheme 2. Control experiments to investigate the reaction pathway shown in Scheme 3.

formation of Ru-dicarbonyl complexes (Figure S51). The six coordinated dicarbonyl complex may serve as an intermediate in an associative pathway under these conditions. Notably, the reaction of complex **1** with ^{13}C-labeled methanol also affirmed the formation of the ^{13}C-labeled mono- and dicarbonyl Ru-complexes (Scheme 2 d). The CO exchange under reaction conditions was finally demonstrated by sequential dehydrogenation of ^{13}C labelled and unlabelled methanol (sections 12.6–12.10 in SI).

Based on these results and previous reports, a plausible catalytic manifold is proposed involving the typical metal-ligand cooperation[20] of MACHO-type ligands (Scheme 3).[17g,21a,b] Complex **1** generates the reactive species Ru^{II} complex (**I**) comprising the cooperative M-N site.[22] Similarly, the manganese complex **6** can enter an analogous manifold upon activation with the base. It is previously well-established that in the presence of alcohol, complex **I** forms the Ru-alcoholate complex **II**.[17d,21a] Complex **II** leads towards the formation of formaldehyde and generates the Ru^{II}-dihydride complex **III** in the first dehydrogenation step. The necessary β-elimination-type C–H bond cleavage at the sp^3 carbon can be associated with a relatively low H/D kinetic isotope effect.[23] Liberation of hydrogen from complex **III** regenerates active species **I**. The decarbonylation of formaldehyde can occur via Ru-complex **IV** to form CO and reconstruct the Ru-hydride complex **III**. In this step, the C–H cleavage has to occur at the sp^2 carbon of the carbonyl group in line with a much larger H/D kinetic isotope effect.[23a] Complex **III** further releases hydrogen to regenerate the active species **I** closing one possible catalytic cycle.

Formaldehyde can also react reversibly with excess methanol to form methoxymethanol, which was detected in the reaction mixture by NMR. On reaction with complex **I**, the half-acetal yields the Ru complex **V** from which dehydrogenation leads to methyl formate, the other experimentally verified intermediate. The resulting Ru-dihydride complex **III** liberates hydrogen and reforms the active species **I**. Methyl formate can also undergo decarbonylation via complex **VI**, similar to complex **IV**. The resulting Ru-methoxy complex **II** provides the molecular linkage between the two alternative cycles.

While the relative contribution of the two cycles cannot be decided at present, the reaction profiles suggest that the dehydrogenation steps prevail in the early stage of the reaction, shortcutting between complexes **I**, **II**, **III** and **I**, **V**, **III**. Once the two organic intermediates, formaldehyde and methyl formate, reach a sufficient concentration, the more demanding decarbonylation steps via **IV** and **VI** are able to compete kinetically, and CO formation starts to catch up.

In conclusion, a catalytic system was developed to generate gas mixtures of carbon monoxide and hydrogen ("syngas") directly from methanol using molecular complexes in the liquid phase. From a series of tested metal complexes, the MACHO-type complexes of Ru^{2+}, [RuH(CO)(BH$_4$)(HN(C$_2$H$_4$PPh$_2$)$_2$)] (**1**), and of Mn^{1+}, [Mn(CO)$_2$(Br)-[HN(C$_2$H$_4$P^{i}Pr$_2$)$_2$] (**6**), revealed the most promising activities.

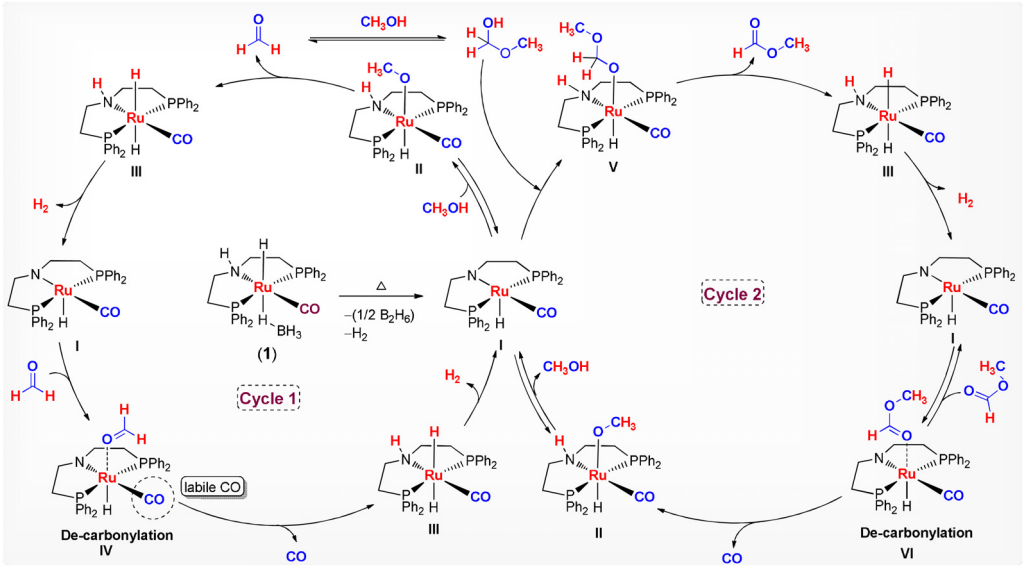

Scheme 3. Postulated catalytic manifold for the dehydrogenation of methanol to carbon monoxide and hydrogen.

With complex **1**, TONs of 3149 and 9232 for CO and H_2 could be achieved, demonstrating the robustness and high productivity of this system. Only trace amounts of CO_2 were formed under these conditions affirming a very high selectivity for the dehydrogenation process. Mechanistic studies revealed that formaldehyde and methyl formate are crucial intermediates in the reaction and demonstrated the importance of the lability of the CO ligand in the catalyst precursor for catalytic turnover. As the initial dehydrogenation is significantly faster than the decarbonylation, the CO/H_2 ratio can vary from very hydrogen-rich to nearly stoichiometric syngas formation ($CO/H_2 = 1:2$). Operating in closed vessels results in significant gas pressures reaching up to 12 bar at reaction temperature or 5 bar at room temperature already in the non-optimized laboratory setup used in this study. This could be beneficial for further use of the gases in energy or chemical applications based on conveniently storable and easily transportable methanol as an additional option for power-to-syngas technologies.

Acknowledgements

We gratefully acknowledge financial support from the Max-Planck Society. The authors thank Emanuele Antico and Niklas Wessel for their helpful suggestions and experimental support, respectively. The studies were performed as part of our activities in the framework of the "Fuel Science Center" funded by the Deutsche Forschungsgemeinschaft (DFG, German Research Foundation) under Germany's Excellence Strategy Exzellenz- cluster 2186, The Fuel Science Center "ID: 90919832". Open access funding was provided by the Max Planck Society. Open Access funding enabled and organized by Projekt DEAL.

Conflict of Interest

The authors declare no conflict of interest.

Keywords: carbon dioxide · carbon monoxide · decarbonylation · dehydrogenation · hydrogen · methanol

[1] a) F. Asinger, *Methanol—Chemie- Und Energierohstoff*, Springer, Berlin, Heidelberg, **1986**; b) G. A. Olah, A. Goeppert, G. K. S. Prakash, *Beyond Oil and Gas: The Methanol Economy*, Wiley-VCH, Weinheim, **2009**; c) M. Bertau, H. Offermanns, L. Plass, F. Schmidt, H.-J. Wernicke, *Methanol: The Basic Chemical and Energy Feedstock of the Future*, Springer-Verlag Berlin Heidelberg, Berlin, **2014**; d) P. Joghee, J. N. Malik, S. Pylypenko, R. O'Hayre, *MRS Energy Sustainability* **2015**, *2*, 3; e) M. Bukhtiyarova, T. Lunkenbein, K. Kahler, R. Schlogl, *Catal. Lett.* **2017**, *147*, 416 – 427; f) W. C. Liu, J. Baek, G. A. Somorjai, *Top. Catal.* **2018**, *61*, 530 – 541; g) Y. T. Liu, D. H. Deng, X. H. Bao, *Chem* **2020**, *6*, 2497 – 2514; h) R. Schlögl, *Angew. Chem. Int. Ed.* **2020**, https://doi.org/10.1002/anie.202007397; *Angew. Chem.* **2020**, https://doi.org/10.1002/ange.202007397.

[2] a) "Production of Hydrogen and Methanol Via Biomass Gasification": E. D. Larson, R. E. Katofsky in *Advances in Thermochemical Biomass Conversion*, Springer Netherlands, Dordrecht, **1993**, pp. 495 – 510; b) "Fossil or Renewable Sources for Methanol Production?": C. Pirola, G. Bozzano, F. Manenti, *Methanol*, Elsevier, Amsterdam, **2018**, pp. 53 – 93.

[3] a) J. Klankermayer, W. Leitner, *Philos. Trans. R. Soc. A* **2016**, *374*, 20150315; b) J. Artz, T. E. Muller, K. Thenert, J. Kleinekorte, R. Meys, A. Sternberg, A. Bardow, W. Leitner, *Chem. Rev.* **2018**, *118*, 434 – 504; c) S. Kar, A. Goeppert, G. K. S. Prakash, *Acc. Chem. Res.* **2019**, *52*, 2892 – 2903; d) X. Jiang, X. Nie, X. Guo, C. Song, J. G. Chen, *Chem. Rev.* **2020**, *120*, 7984 – 8034; e) M. J. Bos, S. R. A. Kersten, D. W. F. Brilman, *Appl. Energy* **2020**, *264*, 114672; f) S. T. Bai, G. De Smet, Y. Liao, R. Sun, C. Zhou, M. Beller, B. U. W. Maes, B. F. Sels, *Chem. Soc. Rev.* **2021**, *50*, 4259 – 4298.

[4] a) G. J. Sunley, D. J. Watson, *Catal. Today* **2000**, *58*, 293 – 307; b) "Acetic Acid": C. Le Berre, P. Serp, P. Kalck, G. P. Torrence, *Ullmann's Encyclopedia of Industrial Chemistry*, Wiley-VCH, Weinheim, **2014**, pp. 1 – 34.

[5] a) J. R. Zoeller, V. H. Agreda, S. L. Cook, N. L. Lafferty, S. W. Polichnowski, D. M. Pond, *Catal. Today* **1992**, *13*, 73 – 91; b) "Acetic Anhydride and Mixed Fatty Acid Anhydrides": H. Held, A. Rengstl, D. Mayer, *Ullmann's Encyclopedia of Industrial Chemistry*, Wiley-VCH, Weinheim, **2014**, pp. 239 – 255.

[6] a) E. Drent, P. H. M. Budzelaar, *Chem. Rev.* **1996**, *96*, 663 – 682; b) "Polyketones: Synthesis and Applications": A. Vavasori, L. Ronchin, *Encyclopedia of Polymer Science and Technology*, Wiley, Hoboken, **2017**, pp. 1 – 41.

[7] "Polycarbonates": *Ullmann's Polymers and Plastics: Products and Processes*, *Vol. 2*, Wiley-VCH, Weinheim, **2016**, pp. 763 – 781.

[8] U. Meier-Westhues, K. Danielmeier, P. Kruppa, E. P. Squiller, *Polyurethanes: Coatings, Adhesives and Sealants*, **2019**.

[9] a) P. W. N. M. van Leeuwen, C. Claver, *Rhodium Catalyzed Hydroformylation*, Kluwer Academic Publishers, Netherlands, **2000**; b) R. Franke, D. Selent, A. Borner, *Chem. Rev.* **2012**, *112*, 5675 – 5732; c) "Hydroformylation": A. M. Trzeciak, *Comprehensive Inorganic Chemistry II*, Elsevier, Amsterdam, **2013**, pp. 25 – 46; d) B. Cornils, W. A. Herrmann, M. Beller, R. Paciello, *Applied Homogeneous Catalysis with Organometallic Compounds: A Comprehensive Handbook in Four Volumes*, 3rd ed., **2017**.

[10] a) M. Beller, *Catalytic Carbonylation Reactions*, *Vol. 18*, Springer-Verlag Berlin Heidelberg, Berlin, **2006**; b) S. T. Gadge, B. M. Bhanage, *RSC Adv.* **2014**, *4*, 10367 – 10389; c) J. B. Peng, H. Q. Geng, X. F. Wu, *Chem* **2019**, *5*, 526 – 552; d) S. L. Zhao, N. P. Mankad, *Catal. Sci. Technol.* **2019**, *9*, 3603 – 3613.

[11] a) C. Liu, T. R. Cundari, A. K. Wilson, *Inorg. Chem.* **2011**, *50*, 8782 – 8789; b) K. Tsuchiya, J. D. Huang, K. Tominaga, *ACS Catal.* **2013**, *3*, 2865 – 2868; c) X. Chen, Y. Chen, C. Song, P. Ji, N. Wang, W. Wang, L. Cui, *Front. Chem.* **2020**, *8*, 709; d) M. González-Castaño, B. Dorneanu, H. Arellano-García, *React. Chem. Eng.* **2021**, *6*, 954 – 976.

[12] S. R. Foit, I. C. Vinke, L. G. J. de Haart, R. A. Eichel, *Angew. Chem. Int. Ed.* **2017**, *56*, 5402 – 5411; *Angew. Chem.* **2017**, *129*, 5488 – 5498.

[13] a) D. R. Palo, R. A. Dagle, J. D. Holladay, *Chem. Rev.* **2007**, *107*, 3992 – 4021; b) S. Sá, H. Silva, L. Brandao, J. M. Sousa, A. Mendes, *Appl. Catal. B* **2010**, *99*, 43 – 57; c) E. Alberico, M. Nielsen, *Chem. Commun.* **2015**, *51*, 6714 – 6725.

[14] a) M. Nielsen, E. Alberico, W. Baumann, H. J. Drexler, H. Junge, S. Gladiali, M. Beller, *Nature* **2013**, *495*, 85 – 89; b) R. E. Rodríguez-Lugo, M. Trincado, M. Vogt, F. Tewes, G. Santiso-Quinones, H. Grützmacher, *Nat. Chem.* **2013**, *5*, 342 – 347; c) P. Hu, Y. Diskin-Posner, Y. Ben-David, D. Milstein, *ACS Catal.* **2014**, *4*, 2649 – 2652; d) J. Campos, L. S. Sharninghausen, M. G. Manas, R. H. Crabtree, *Inorg. Chem.* **2015**, *54*, 5079 – 5084; e) K.

Fujita, R. Kawahara, T. Aikawa, R. Yamaguchi, *Angew. Chem. Int. Ed.* **2015**, *54*, 9057 – 9060; *Angew. Chem.* **2015**, *127*, 9185 – 9188.

[15] a) E. Alberico, P. Sponholz, C. Cordes, M. Nielsen, H. J. Drexler, W. Baumann, H. Junge, M. Beller, *Angew. Chem. Int. Ed.* **2013**, *52*, 14162 – 14166; *Angew. Chem.* **2013**, *125*, 14412 – 14416; b) E. A. Bielinski, M. Forster, Y. Y. Zhang, W. H. Bernskoetter, N. Hazari, M. C. Holthausen, *ACS Catal.* **2015**, *5*, 2404 – 2415; c) M. Andérez-Fernández, L. K. Vogt, S. Fischer, W. Zhou, H. Jiao, M. Garbe, S. Elangovan, K. Junge, H. Junge, R. Ludwig, M. Beller, *Angew. Chem. Int. Ed.* **2017**, *56*, 559 – 562; *Angew. Chem.* **2017**, *129*, 574 – 577; d) Z. Shao, Y. Li, C. Liu, W. Ai, S. P. Luo, Q. Liu, *Nat. Commun.* **2020**, *11*, 591.

[16] a) W. J. Shen, Y. Matsumura, *Phys. Chem. Chem. Phys.* **2000**, *2*, 1519 – 1522; b) Y. Y. Liu, T. Hayakawa, T. Ishii, M. Kumagai, H. Yasuda, K. Suzuki, S. Hamakawa, K. Murata, *Appl. Catal. A* **2001**, *210*, 301 – 314; c) J. C. Brown, E. Gulari, *Catal. Commun.* **2004**, *5*, 431 – 436; d) S. A. Ranaweera, W. P. Henry, M. G. White, *ACS Omega* **2017**, *2*, 5949 – 5961; e) G. J. Li, C. T. Gu, W. B. Zhu, X. F. Wang, X. F. Yuan, Z. J. Cui, H. L. Wang, Z. X. Gao, *J. Cleaner Prod.* **2018**, *183*, 415 – 423.

[17] a) E. Balaraman, C. Gunanathan, J. Zhang, L. J. Shimon, D. Milstein, *Nat. Chem.* **2011**, *3*, 609 – 614; b) D. Shen, D. L. Poole, C. C. Shotton, A. F. Kornahrens, M. P. Healy, T. J. Donohoe, *Angew. Chem. Int. Ed.* **2015**, *54*, 1642 – 1645; *Angew. Chem.* **2015**, *127*, 1662 – 1665; c) P. Daw, Y. Ben-David, D. Milstein, *J. Am. Chem. Soc.* **2018**, *140*, 11931 – 11934; d) A. Kaithal, M. Schmitz, M. Hölscher, W. Leitner, *ChemCatChem* **2019**, *11*, 5287 – 5291; e) D. J. Braden, R. Cariou, J. W. Shabaker, R. A. Taylor, *Appl. Catal. A* **2019**, *570*, 367 – 375; f) J. Sklyaruk, J. C. Borghs, O. El-Sepelgy, M. Rueping, *Angew. Chem. Int. Ed.* **2019**, *58*, 775 – 779; *Angew. Chem.* **2019**, *131*, 785 – 789; g) A. Kaithal, P. van Bonn, M. Hölscher, W. Leitner, *Angew. Chem. Int. Ed.* **2020**, *59*, 215 – 220; *Angew. Chem.* **2020**, *132*, 221 – 226; h) M. Schlagbauer, F. Kallmeier, T. Irrgang, R. Kempe, *Angew. Chem. Int. Ed.* **2020**, *59*, 1485 – 1490; *Angew. Chem.* **2020**, *132*, 1501 – 1506; i) P. Schlichter, C. Werlé, *Synthesis* **2021**, https://doi.org/10.1055/a-1657-2634.

[18] For comparison, a pincer complex with Mn in the oxidation state +2, $[MnCl_2[HN(C_2H_4P^iPr_2)_2]]$ (**9**), was synthesized and tested for dehydrogenation of methanol. In line with the presumes Ru^{2+}/Mn^{1+} analogy, this complex did not show any reactivity towards the formation of CO and H_2. For the synthesis of complex **9**, see reference: S. Elangovan, C. Topf, S. Fischer, H. Jiao, A. Spannenberg, W. Baumann, R. Ludwig, K. Junge, M. Beller, *J. Am. Chem. Soc.* **2016**, *138*, 8809 – 8814.

[19] N. Matubayasi, M. Nakahara, *J. Chem. Phys.* **2005**, *122*, 074509.

[20] a) J. R. Khusnutdinova, D. Milstein, *Angew. Chem. Int. Ed.* **2015**, *54*, 12236 – 12273; *Angew. Chem.* **2015**, *127*, 12406 – 12445; b) B. Chatterjee, W. C. Chang, S. Jena, C. Werlé, *ACS Catal.* **2020**, *10*, 14024 – 14055; c) M. R. Elsby, R. T. Baker, *Chem. Soc. Rev.* **2020**, *49*, 8933 – 8987.

[21] a) A. Kaithal, M. Schmitz, M. Hölscher, W. Leitner, *ChemCatChem* **2020**, *12*, 781 – 787; b) A. Kaithal, C. Werlé, W. Leitner, *JACS Au* **2021**, *1*, 130 – 136.

[22] B. Chatterjee, W. C. Chang, C. Werlé, *ChemCatChem* **2021**, *13*, 1659 – 1682.

[23] a) N. Sieffert, R. Reocreux, P. Lorusso, D. J. Cole-Hamilton, M. Buhl, *Chem. Eur. J.* **2014**, *20*, 4141 – 4155; b) H. T. Abdulrazzaq, A. R. Chokanlu, B. G. Frederick, T. J. Schwartz, *ACS Catal.* **2020**, *10*, 6318 – 6331.

Manuscript received: August 13, 2021
Revised manuscript received: September 23, 2021
Accepted manuscript online: October 1, 2021
Version of record online: November 16, 2021

